Hard repulsive barrier in hot adatom motion during dissociative adsorption of oxygen on Ag(100)

Ming-Feng Hsieh, Deng-Sung Lin, Heiko Gawronski, and Karina Morgenstern

Citation: The Journal of Chemical Physics **131**, 174709 (2009); doi: 10.1063/1.3258849
View online: http://dx.doi.org/10.1063/1.3258849
View Table of Contents: http://scitation.aip.org/content/aip/journal/jcp/131/17?ver=pdfcov
Published by the AIP Publishing

Hard repulsive barrier in hot adatom motion during dissociative adsorption of oxygen on Ag(100)

Ming-Feng Hsieh,[1] Deng-Sung Lin,[1] Heiko Gawronski,[2] and Karina Morgenstern[2,a)]
[1]*Institute of Physics, National Chiao Tung University, 1001 Ta-Hsueh Road, Hsinchu 30010, Taiwan and Department of Physics, National Tsing Hua University, 101 Kuang-Fu Road Section 2, Hsinchu 30013, Taiwan*
[2]*Division of Atomic and Molecular Structures (ATMOS), Institut for Solid State Physics, Leibniz University of Hannover, Appelstraße 2, D-30167 Hannover, Germany*

(Received 18 June 2009; accepted 14 October 2009; published online 6 November 2009)

Random pairing simulation and low temperature scanning tunneling microscopy (STM) are used to investigate the detailed O_2 dissociative adsorption processes at 200 K for various coverages. The distribution of oxygen adatoms shows a strong repulsion between the adsorbates with a radius of ~0.8 nm. The comparison between STM results and simulation reveals two prominent pairing distances of 2 and 4 nm and their branching ratio is about 2:1. These findings shed new light on the origin of the large intrapair distances found and on the process behind the empirical "eight-site rule." © *2009 American Institute of Physics*. [doi:10.1063/1.3258849]

I. INTRODUCTION

The adsorption of oxygen on silver single-crystal surfaces has been widely studied in the past decades.[1–6] This interest arises because oxygen chemisorbs on silver systems in both atomic and molecular form and thus allows molecular dissociation to be studied at a fundamental level. Moreover, the silver oxygen interaction is of enormous industrial relevance. It is a familiar catalyst for epoxidation of ethylene to ethylene oxide ($C_2H_4+O \rightarrow C_2H_4O$) and the partial oxidation of methanol to formaldehyde ($CH_3OH+O \rightarrow CH_2O+H_2O$).[7,8] The microscopic understanding of oxygen adsorption and dissociation is a prerequisite to understand the catalytic cycle. Thereby, the distribution of the oxygen atoms as educts for further reactions is of particular relevance. The identification of the catalytically active oxygen species on silver surfaces was consequently the subject of numerous studies.[1,9,10] Finally, the oxidation process is interesting because silver oxide nanoclusters were shown to be potential candidates for optical memories.[11]

Three oxygen adsorbed states of oxygen on Ag(001) were reported: (1) a physisorbed molecular species,[12,13] (2) a chemisorbed molecular species[3] below 130 K that forms two-dimensional $c(4\times2)$ islands,[14] and (3) a dissociative (atomic) chemisorbed oxygen state above 130 K with a very low sticking coefficient S of 7.4×10^{-4} at T=150 K and 1.3×10^{-4} at T=250 K.[15] After oxygen exposure on the Ag(001) surface at 180 K, low energy electron diffraction (LEED) measurement exhibited a $c(2\times2)$ pattern,[1] and heating from 180 K to room temperature led to a structural transition from $c(2\times2)$ to $p(1\times1)$. A combined scanning tunneling microscopy (STM), LEED, and Auger electron spectroscopy (AES) study revealed the complete complex phase diagram with a variety of different structures depending on partial pressure and temperature.[10]

At very low coverage, Schintke *et al.*[4] first reported hot adatom motion on this surface as obvious from a pairing of O-adatoms over two distinct and large intrapair distances around 2 nm (± 0.4 nm) and 4 nm (± 0.4 nm) after exposing the Ag(001) surface to oxygen at 140 K. These distances correspond to 7 and 14 surface lattice constants (SLCs) of 0.289 nm on Ag(001). There is ample evidence that the oxygen transients are important in a wide range of catalytic surface reactions.[16] Previous STM studies on this topic focused on the pair distribution revealing average intrapair distances that range from ~2 to ~14 SLCs.[17–20] Because of the large separation of the adsorbates at low coverage under study, an effect of the adsorbate-adsorbate interaction on the transient ballistic motions of "hot" adatoms has not yet been investigated and thermal motions of adatoms cannot be completely ruled out.

In this article, we investigate the dissociation of oxygen on Ag(100) at a higher sample temperature of 200 K and a three-times larger coverage of ~1.7% ML than in the previous study.[4] At this coverage, the separation of the atoms is smaller than the paring distances observed before at 140 K, allowing the examination of interactions between adsorbates and dissociated fragments. The ~40% higher sample temperature also provides a mean to differentiate the transient motions of the adsorption fragments from the thermal motions. We compare the distribution of adatoms found in STM images acquired at 5 K to simulations of random pair distributions. A hard repulsive interaction between the oxygen atoms is found to limit the nearest neighbor distance to 0.8 nm. The comparison of simulation and LT-STM results reveals pairing distances of ~2 nm and ~4 nm with a ratio of 2:1. This result sheds new light on the large intrapair distances found and on the process behind the empirical "eight-site rule." This empirical rule excludes the adsorption of the second atom of a dissociated molecule at the eight neighboring sites of the first atom.[21]

a)Author to whom correspondence should be addressed. Electronic mail: morgenstern@fkp.uni-hannover.de.

II. EXPERIMENTAL DETAILS

The experiments were performed with a custom-built low-temperature STM in a ultra-high vacuum (UHV) system with a base pressure below 5×10^{-10} mbar.[22] The single crystal Ag(001) surface is cleaned by cycles of Ar^+ sputtering (3.7 μA, 0.55 keV, 25 min) and annealing (900 K, 3 min). We adsorb oxygen from the background pressure measured by a cold cathode gauge close to the gas inlet to 1×10^{-5} mbar and by a hot filament gauge in the main chamber to 2×10^{-6} mbar. The surface is thereby held at (200 ± 5) K. At this temperature adsorption is dissociative.[1] Exposure to 300 and 900 L O_2 leads to an O coverage of 0.6% and 1.7% ML, respectively, as determined in the STM. A monolayer refers to the surface density of silver atoms in the (001) plane (1 ML $=1.2\times10^{15}$ atoms/cm^{-2}).

The sample is then transferred into the cold shields of the cryostat, where all STM measurements are performed at 5 K. For image calibration the standard method of atomic resolution of the native surface has been employed. STM images are measured in the constant-current mode at the parameters given in the figure captions. Apart from a plane subtraction and a low pass filter no further image processing has been employed. The conventional gray scale representation implies that depressions/protrusions in the STM image correspond to a reduced/enhanced local density-of-states (LDOS). Based on comparison to atomic resolution images (see below) the precision of the distance between two atoms is better than 0.1 nm.

In order to analyze the distance distributions extracted from the STM images, we performed random pairing (RP) simulations. On a rectangle of the size of the STM image, the program randomly places the number of atoms as determined from the STM images according to the following rules to include the origin of two atoms from one molecule and the repulsion between adatoms. If a randomly selected site for the first oxygen adatom from a pair is less than 0.8 nm away from a previously adsorbed adatom, no adsorption is allowed and a new site is chosen randomly. The previous report for dissociation at 140 K observed a distribution of ±0.4 nm around the mean distances D.[4] We attribute this distribution mainly to the discrete nature of the adsorption sites of the oxygen atoms in a fourfold hollow sites (see below), which have a maximum distance of $\sqrt{2}SLC=0.4$ nm in $\langle100\rangle$ direction. The distance of the second oxygen adatom released from the O_2 molecule to the first one is thus chosen randomly between $(D-0.4)$ nm and $(D+0.4)$ nm. The direction of the second oxygen adatom traveling away from the first one is also generated randomly. Again, if the second adatom would sit too close to an occupied site (distance less than 0.8 nm), both the distance and the direction for the second adatom are regenerated.

The standard deviation σ is used for a quantitative analysis comparing the results from the STM measurement with those from the computer simulations for variant hypothetical pairing distances. Each simulation data point used for the standard deviation is the average value of 50 simulation runs.

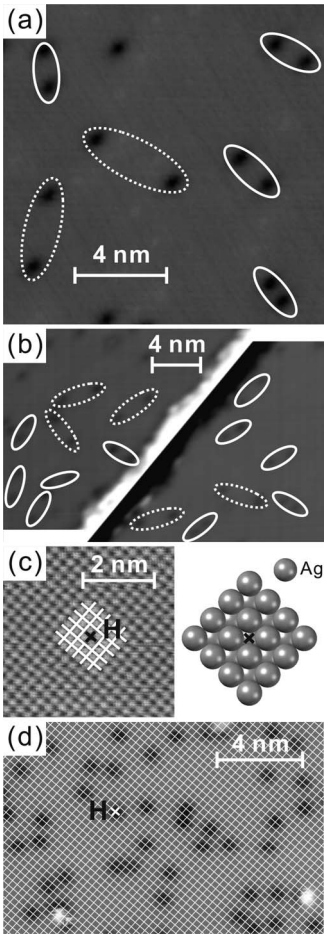

FIG. 1. STM images of Ag(001) surface [(a) and (b)] with an O coverage of 0.6% ML; pairs are marked by ellipses ($V_{\text{tunnel}}=-100$ mV, $I_{\text{tunnel}}=10$ pA); image in (b) is split close to the step edge and different contrasts are chosen for the two terraces in order to make the atoms visible on both sides of the step edge (c) native substrate in atomic resolution, ($V=-21$ mV, $I=4.6$ nA) with ball model showing most stable adsorption site of an oxygen atom calculated in Ref. 4; white lines show lattice intervals (d) STM image of surface with an O coverage of 1.7% ML; superimposed atomic grid deduced from atomic resolution, ($V=-150$ mV, $I=78$ pA); crosses in (c) and (d) indicate fourfold hollow site H.

III. RESULTS

After exposing the Ag(001) surface to O_2 at 200 K, isolated oxygen atoms are observed as circular depressions with a diameter of ~0.6 nm in the STM image [Figs. 1(a), 1(b), and 1(d)]. In agreement with earlier STM results and Green's function STM image calculations,[14] the depression reflects the reduced LDOS of the four surrounding Ag atoms induced by an oxygen atom adsorbed in a hollow site as compared to the LDOS of the unperturbed Ag atoms. Especially at low coverage, e.g., 0.6% ML in Fig. 1(a), a pairing of the oxygen adsorbates is obvious. Two main intrapair distances distributed around 2.0 and 4.0 nm (corresponding to about 7 and 14 SLCs) are found, exemplified in Figs. 1(a) and 1(b) as ellipse and dashed ellipse, respectively. This qualitative picture is quantitatively confirmed below. Such a pair of atoms originates from the dissociation of a single adsorbing molecule and the subsequent motion of the formed adatoms. Also this observation is in agreement with earlier work[4] performed at lower temperature (140 K) and over a variety of coverages (0.1%–0.5% ML).

Results obtained by indirect means from high resolution electron energy loss spectroscopy showed an increase in dissociation probability on the stepped Ag(410) surface.[3] If this increase was based on an enhanced sticking probability at step edges, it would imply a larger density of oxygen atom pairs near step edges than on terraces. However, in our STM images, e.g., in Fig. 1(b), the oxygen atom pairs are evenly distributed over the surface and no preference close to step edges is found. Thus, the higher dissociation probability cannot be related to the fact that the oxygen dissociates on Ag(001) only if the molecules are bound to kink sites at step edges. We suggest that the change in electronic structure on small terraces is at the origin of the enhanced dissociation probability on Ag(410).[23]

The atomic resolution of the surface [Fig. 1(c)] superimposed over an image with oxygen atoms at a larger coverage of ~1.7% ML [Fig. 1(d)] demonstrates that all atoms are adsorbed in equivalent adsorption sites. According to theory[4] this is the fourfold hollow site [Fig. 1(c)]. In conclusion, Fig. 1 demonstrates that at 200 K the oxygen atoms separate in a hot adatom motion after dissociation on the terrace and accommodate in the fourfold hollow site. Here, we investigate their nonthermal motion further at the higher coverage.

At this higher oxygen coverage [see Fig. 2(a)], the pairing of oxygen adatoms is not as easily revealed because pairs may overlap with others and the oxygen atoms seem to be randomly distributed over the Ag(001) surface. To analyze the oxygen atom pair distribution, we present a two-dimensional (2D) radial distribution plot as shown in Fig. 2(f) for the STM image in Fig. 2(a). For this plot we determine for each atom the direction and distance of each other atom within 3 nm. Such a pair is then represented by a dot at the distance from the center of the image in the observed direction. The same distance and direction can of course occur more than once and in the graph the density of a distance/direction pair is visualized by gray levels where darker areas reflect higher densities. Note that in this procedure each distance is counted twice and the pair distribution plot shows an inversion symmetry. The shortest distance of 0.6 nm (about 2 SLCs) is only observed for one pair, otherwise, the pair distances are larger than 0.8 nm (about $2\sqrt{2}$ SLCs), which is shown as a circle of radius 0.8 nm in Figs. 2(f)–2(j). The minimal distance found here after transient motion equals the nearest neighbor distance found in a STM study within small islands showing $p(2\times2)$ superstructure after high dosage of O_2 ($\approx10^{10}$ L) on the Ag(001) surface at 300 K, i.e., after thermal motion.[10]

We now analyze the experimental 2D radial distribution plot by comparing it to simulated distributions. Figure 2(b) displays a simulation for a totally random distribution of the same oxygen coverage as in Fig. 2(a) on the same size of the STM image. Its 2D radial distribution plot is shown in Fig. 2(g). This distribution clearly disagrees with the experimental distribution. In particular, the repulsive ring is not reproduced. Therefore, we include a repulsion restricting the distance to 0.8 nm (~$2\sqrt{2}$ SLCs) into the random simulation. The result is shown in Fig. 2(c). Its radial distribution map in Fig. 2(h) reproduces the STM result much better.

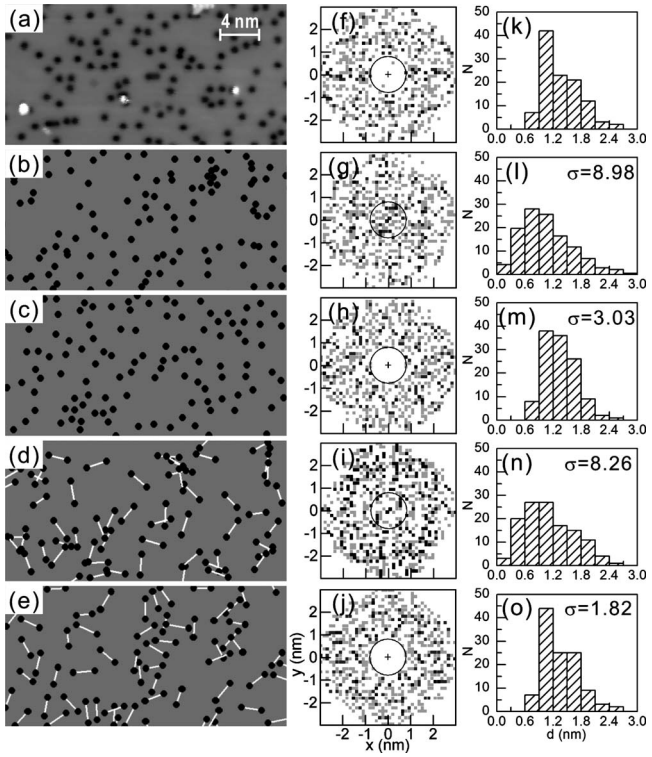

FIG. 2. (a) STM image of the Ag(001) surface with 1.7% ML coverage ($V=-150$ mV, $I=78$ pA). [(b)–(d)] Examples for the simulations with the same oxygen coverage as in (a). The black dots indicate oxygen atoms. Totally random simulations are shown in (b) without repulsion and in (c) with repulsion limiting the nearest neighbor distance to ≥0.8 nm. RP simulation for pairs with distances of (2.0 ± 0.4) nm are shown in (d) without repulsion and (e) with a minimum nearest neighbor distance of ≥0.8 nm. The white lines connect oxygen atom pairs. [(f)–(j)] Plot of the 2D pair distribution function within a radius of 3 nm with respect to each atom from (a)–(e). The distance between two pixels is 0.15 nm, about half a SLC, and the radius of small circle is 0.8 nm. [(k)–(o)] Histograms of the nearest neighbor distance from (a) to (e). Standard deviations for each case are labeled.

We next discuss whether inclusion of the pairing of the O-adatoms as observed in Fig. 1 into the simulation leads to an even better mimicking of the experiment than the repulsion. A RP simulation with pair distances of (2.0 ± 0.4) nm without exclusion zone is shown in Fig. 2(d), its 2D radial distribution plot in Fig. 2(i). Both Figs. 2(i) and 2(n) seem very similar to the simulation of totally random in Figs. 2(g) and 2(l).

Finally, we include both effects in our simulation. A RP simulation with pair distances of (2.0 ± 0.4) nm with repulsion is shown in Fig. 2(e), its 2D radial distribution plot in Fig. 2(j). It is not obvious, whether this distribution [Fig. 2(j)] or the one presented in Fig. 2(h) better reproduces the experimental distribution in Fig. 2(f).

The directions of the pairs are random and thus we now concentrate on the distances only. Figures 2(k)–2(o) display histograms of the nearest neighbor distance for a measured area of 26×26 nm^2 for the experimental and the four simulated distributions shown in Figs. 2(a)–2(e) and the same oxygen coverage of 1.7% ML. Again, the simulations that do not take into account the repulsive ring [Figs. 2(l) and 2(n)] do not reproduce the experiment [Fig. 2(k)]. The distribution that considers the repulsive ring only [Fig. 2(m)] resembles

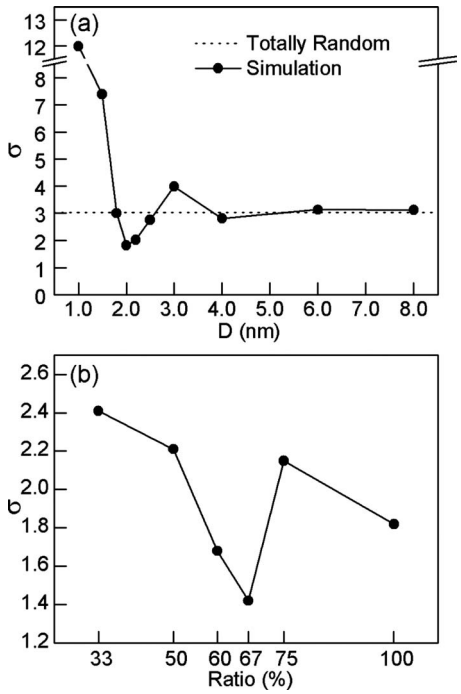

FIG. 3. Standard deviations σ of nearest-neighbor distances of RP simulation to STM results for different pairing distances: (a) for one pairing distance D (b) in dependence of ratio of 2 nm ($\pm$0.4 nm) to 4 nm ($\pm$0.4 nm) pairs.

the experiment less well than the one that also considers pairing distances of (2.0 ± 0.4) nm [Fig. 2(o)]. Therefore, despite the larger coverage the origin of two atoms from one molecule, i.e., the pairing, is still detectable.

For a quantitative analysis, we compare the results from the STM measurement to those from the computer simulations via the standard deviation σ defined as

$$\sigma = \sqrt{\frac{1}{n}\sum_{i=1}^{n}(N_{Sim,i} - \overline{N_{\mathrm{STM},i}})^2},$$

where N indicates the number within an interval i for the nearest neighbor distance distribution of the oxygen atoms and n indicates the total number of intervals. The smaller σ the better the STM measurement is simulated. The simulations in Figs. 2(b)–2(e) give standard deviations of 8.98, 3.03, 8.26, and 1.82 and thus confirm that both, the repulsive ring and the pairing improve the mimicking of the experimental distribution.

In order to determine the underlying paring distance, variant distances [1.0, 1.5, 1.8, 2.0, 2.2, 2.5, 3.0, 4.0, 6.0, and 8.0 nm ($\pm$0.4 nm)] and the random distribution are simulated and compared to the related STM data. For all pairing distances the repulsive ring was included. Figure 3(a) shows that for pairing distances above 4 nm the pairing distribution cannot be discriminated from a random distribution. Most importantly, the best fit of simulation to STM results is found for pairing distances of 2.0 ($\pm$ 0.4) nm.

Finally, we include the larger pairing distance of 4 nm found in Fig. 1 and also at 140 K into the simulation.[4] Thereby, we vary the ratio of 2–4 nm pairs. The percentages of 33, 50, 60, 67, and 75 indicate that the ratios of 2 nm pairs : 4 nm pairs are 1:2, 1:1, 3:2, 2:1, and 3:1, and 100% denotes only 2 nm pairs. We caution that with increasing coverage the probability increases that a molecule approaches an adsorption modified surface site and thus may follow a completely different dissociation path, possibly connected with yet another pairing distance not included in our analysis. As one adsorbed molecule modifies the LDOS of four silver atoms,[4] we estimate this to be an effect of the order of 3% –4% for the coverage investigated here. Within this error margin, the comparison of experiment to simulation reveals that the pairing distance has a ratio of 2:1 for 2–4 nm pairs [Fig. 3(b)].

IV. DISCUSSION

On a conceptual level, our study demonstrates that at a coverage, where atom pairs are no longer well separated, the origin of two atoms from one molecule, i.e., the pairing, is still detectable. This extents the possibility of STM to investigate the hot adatom motion beyond single or well separated pairs. Only at this larger coverage the depletion region around each adsorbed atom with no atoms closer than 0.6 nm (about 2 SLCs) and the nearest neighbor distances mostly larger than 0.8 nm (about $2\sqrt{2}$ SLCs) is detectable. Such a depletion region implies repulsion in the adatom interaction. Indeed, density functional theory (DFT) calculation showed that a repulsive barrier leads to a saturation coverage of oxygen on silver of 0.24 ML only[24] consistent with $p(2\times2)$ superstructure found experimentally on Ag(100) at higher coverage.[10] Most likely, such a repulsion results from a partial charge transfer from the surface to the adatoms. A recent DFT study calculated this charge transfer for oxygen molecules in dependence of the work function change upon adsorption for a variety of metals, but not silver.[25,26] This study allows to estimate this charge transfer to be approximately 0.18 electrons for the molecule on Ag(111). A density functional calculation on Ag(110) suggests also a charge transfer from the metal to the adsorbed oxygen atom.[27] Based on these studies, it is reasonable to assume a partial charge transfer also to the oxygen atom on Ag(100). This holds for the atom that is already equilibrated. For a repelling interaction, in addition the atom in transient motion should be charged. This is possible via the so-called harpooning mechanism that was found to be rate limiting in the dissociative adsorption of oxygen on Ag(110) and Ag(111).[28,29] In this process an electron attaches to the oxygen molecule to form an ion, while the molecule is still quite far away from the surface. For substrates with low work functions this electron can further be emitted into the vacuum and was measured.[30] Here, the work function of silver will not allow to do so, and the charge might only be transferred back to the metal after the transient motion. The origin of the depletion region is thus electrostatic interaction.

Furthermore, the depletion region might also be related to the so-called eight-site rule.[21] The eight-site rule is an empirical rule that excludes the adsorption of the second atom of a dissociated molecule at the eight neighboring sites. A physical explanation for this rule was not provided. Our results suggest that this depletion region is not the result of a

separation of the atoms originating from the same molecule. Instead, one of the adatoms is already settled on the surface, the other one is still mobile and is not allowed to approach the adatom too closely because of electrostatic repulsion.

Further implications of our study for the understanding of hot adatom motion result from the temperature independence of the pairing distances and distance ratio. An adatom separation measured at one temperature only[4] could still have been explained by a thermal motion during deposition. However, the same separations found at ~40% higher temperature as observed here cannot be explained by a thermal motion in view of the exponential temperature dependence of a thermally induced random motion of adparticles. The distances found thus reflect the dissociation process at or close to the Ag(001) surface. Furthermore, the temperature-independent distance ratio excludes one of the two possibilities discussed before for the two pairing distances.[4] The different distances thus may not result from either a molecule dissociating upon approach or equilibrating as a molecule. The latter should be negligible at 200 K and in any case the ratio of these processes is expected to be temperature dependent. Indeed, an independent annealing experiment of molecules adsorbed at 100 K, which desorb from defect-free terrace sites already between 130 and 160 K, supports this conclusion. As no calculations for Ag(100) exist, we discuss the results qualitatively in light of recent calculations on Al(111), although the energy gain upon dissociation differs on the two surfaces. A nonadiabatic quantum dynamical calculation[31] for oxygen dissociation over Al(111) provides two possible dissociation processes named indirect dissociation and ballistic dissociation. In the ballistic case, all energies, which are originally equally distributed between the atoms, are almost completely transferred to the moving atom by momentum transfer due to repulsive forces. The two different processes originate from the differing orientations of the molecular axis with respect to the surface normal during approach. Thus, it is more likely that the two different pair distances are connected to two different predominant dissociation events A and B. In A the dissociation energy E_{dis} is distributed equally between the two adatoms (initial energy $E_A = E_{dis}/2$), while in the other one the dissociation energy is predominantly transferred to one of the two adatoms ($E_B = E_{dis}$). As the diffusion distance of an adatom increases with its initial energy E as $\sim E^{1.6}$ this could explain the two different distances.[32] Such a scenario should not be restricted to Al(111), although the branching ratio will depend on the exact potential energy surface and thus differ on Ag(100).

However, also the repulsive barrier sheds new light on the process of hot adatom motion. The adatoms are during the dissociation process initially closer than this barrier and thus their initial motion either along the surface or in a cannonball-like trajectory will be accelerated by the electrostatic repulsion, possibly even aiding or affording a cannonball-like dissociation. The charge distribution between the two atoms would need nonadiabatic quantum dynamics calculations as were employed for NO.[33] If the charged states are not the same for all dissociated O_2 molecules this might be a further possibility to explain the two different distances observed.

V. CONCLUSIONS

We investigate terrace dissociation of oxygen on Ag(100) at 200 K and at coverages up to 1.7% ML. The results generalize earlier reports for dissociation at 140 K and coverages below 0.5% ML. Through comparison with RP simulations we reveal pairing distances of 2 nm (±0.4 nm) and 4 nm (±0.4 nm) with a ratio of 2:1. A repulsive barrier found suggests that both the equilibrated atoms and the ones in transient motion are charged. We suggest that this transient repulsion is at the origin of the empirical "eight-site rule." This charging sheds new light on the origin of the unusually large adatom distances found between the oxygen atoms after oxygen dissociation on Ag(001) and opens further explanations for the two distinct distances.

ACKNOWLEDGMENTS

The authors wish to acknowledge the financial support of the Sandwich Program sponsored by the German Academic Exchange Service (DAAD) and the National Science Council, Taiwan. Discussions with Jörg Meyer, FHI Berlin, are gratefully acknowledged. We thank Carsten Sprodowski, Leibniz University of Hannover, for experimental support and for providing Fig. 1(c).

[1] C. S. A. Fang, Surf. Sci. **235**, L291 (1990).
[2] P. A. Gravil, D. M. Bird, and J. A. White, Phys. Rev. Lett. **77**, 3933 (1996).
[3] F. B. de Mongeot, A. Cupolillo, U. Valbusa, and M. Rocca, Chem. Phys. Lett. **270**, 345 (1997).
[4] S. Schintke, S. Messerli, K. Morgenstern, J. Nieminen, and W.-D. Schneider, J. Chem. Phys. **114**, 4206 (2001).
[5] J. R. Hahn and W. Ho, J. Chem. Phys. **123**, 214702 (2005).
[6] M. Alducin, H. F. Busnengo, and R. D. Muino, J. Chem. Phys. **129**, 224702 (2008).
[7] V. I. Bukhtiyarov, V. V. Kaichev, E. A. Podgornov, and I. P. Prosvirin, Catal. Lett. **57**, 233 (1999).
[8] R. J. Beuhler, R. M. Rao, J. Hrbek, and M. G. White, J. Phys. Chem. B **105**, 5950 (2001).
[9] G. Cipriani, D. Loffreda, A. Dal Corso, S. de Gironcoli, and S. Baroni, Surf. Sci. **501**, 182 (2002).
[10] I. Costina, M. Schmid, H. Schiechl, M. Gajdos, A. Stierle, S. Kumaragurubaran, J. Hafner, H. Dosch, and P. Varga, Surf. Sci. **600**, 617 (2006).
[11] L. A. Peyser, A. E. Vinson, A. P. Bartko, and R. M. Dickson, Science **291**, 103 (2001).
[12] O. Citri, R. Baer, and R. Kosloff, Surf. Sci. **351**, 24 (1996).
[13] M. Schmidt, A. Masson, and C. Brechignac, Phys. Rev. Lett. **91**, 243401 (2003).
[14] S. Messerli, S. Schintke, K. Morgenstern, J. Nieminen, and W.-D. Schneider, Chem. Phys. Lett. **328**, 330 (2000).
[15] M. Rocca, L. Savio, L. Vattuone, U. Burghaus, V. Palomba, N. Novelli, F. Buatier de Mongeot, U. Valbusa, R. Gunnella, G. Comelli, A. Baraldi, S. Lizzit, and G. Paolucci, Phys. Rev. B **61**, 213 (2000).
[16] A. F. Carley, P. R. Davies, and M. W. Roberts, Catal. Lett. **80**, 25 (2002).
[17] J. Wintterlin, R. Schuster, and G. Ertl, Phys. Rev. Lett. **77**, 123 (1996).
[18] U. Diebold, W. Hebenstreit, G. Leonardelli, M. Schmid, and P. Varga, Phys. Rev. Lett. **81**, 405 (1998).
[19] M. K. Rose, A. Borg, J. C. Dunphy, T. Mitsui, D. F. Ogletree, and M. Salmeron, Surf. Sci. **561**, 69 (2004).
[20] T. Zambelli, J. V. Barth, J. Wintterlin, and G. Ertl, Nature (London) **390**, 495 (1997).
[21] C. R. Brundle, J. Behm, and J. A. Barker, J. Vac. Sci. Technol. A **2**, 1038 (1984).
[22] M. Mehlhorn, H. Gawronski, L. Nedelmann, A. Grujic, and K. Morgenstern, Rev. Sci. Instrum. **78**, 033905 (2007).
[23] K. Morgenstern, K.-F. Braun, and K.-H. Rieder, Phys. Rev. Lett. **89**,

226801 (2002).
[24] M. Todorova, W. X. Li, M. V. Ganduglia-Pirovano, C. Stampfl, K. Reuter, and M. Scheffler, Phys. Rev. Lett. **89**, 096103 (2002).
[25] L. Qi, X. Qian, and J. Li, Phys. Rev. Lett. **101**, 146101 (2008).
[26] C. Q. Sun, Appl. Surf. Sci. **246**, 6 (2005).
[27] F. E. Olsson, N. Lorente, and M. Persson, Surf. Sci. **522**, L27 (2003).
[28] M. Dean and M. Bowker, Appl. Surf. Sci. **35**, 27 (1988).
[29] P. H. F. Reijnen, A. Raukema, U. van Slooten, and A. W. Kleyn, Surf. Sci. **253**, 24 (1991).
[30] G. C. Poon, T. J. Grassman, J. C. Gumy, and A. C. Kummel, J. Chem. Phys. **119**, 9818 (2003).
[31] G. Katz, R. Kosloff, and Y. Zeiri, J. Chem. Phys. **120**, 3931 (2004).
[32] Y. Zeiri, J. Chem. Phys. **112**, 3408 (2000).
[33] G. Katz, Y. Zeiri, and R. Kosloff, J. Phys. Chem. B **109**, 18876 (2005).